

COMPACT PROTON AND CARBON ION SYNCHROTRONS FOR RADIATION THERAPY

K. Endo*, Z. Fang, KEK, Tsukuba, Japan

S. Fukumoto, M. Mizobata, A. Teramoto, Y. Ishi, Mitsubishi ElectricCo., Kobe, Japan

G.I. Silvestrov, I.I. Averboukh, BINP, Novosibirsk, Russia

Abstract

A compact proton and carbon ion synchrotron development program is approved in 2001 to promote the advanced radiation treatment by developing a suitable medical accelerator adopting new technologies. They depend on the high magnetic field to make the ring as small as possible. The maximum proton (carbon ion) energy is 200 MeV (300 MeV/u) with the circumference of 12 m (16m) at the maximum dipole field of 3 T (4 T). Main concerns of this manuscript are the development of a high field magnet with a uniform field distribution and a short high voltage broadband RF cavity. Three dimensional transient field calculations were carried out under the pulse excitation with the rise time of 5 ms and the beam behaviours are also simulated under the sextupole error field in the dipoles. Beam optics and transverse beam stability studies are presented including the lattice design.

1 INTRODUCTION

Since it is recognized that the proton and heavy ion particle accelerators are an efficient tool to cure a malignant tumor, many efforts are being taken to make them compact with improved therapeutic functions to meet the medical treatment device [1-3]. In disregard of their superior localization of the radiation dose to the tumor, their installations at the hospitals are limited probably due to a large initial investment and running costs. This development program aims to reduce these costs and to popularize the proton and/or heavy ion accelerator-based therapeutics by making the synchrotron compact.

2 LATTICE DESIGN

The proton and heavy ion are accelerated in the individual rings because the charge to mass ratio is different and each requires the different bending radius to realize the optimized ring [4].

2.1 Lattice of the proton ring

It is planned to adopt a low cost 2 MeV RFQ linac to reduce the overall cost. The low energy injection causes the large beam excursion at the initial stage of acceleration by the momentum swing due to the synchrotron oscillation. It is desirable to design the lattice with small dispersion function as well as small vertical and horizontal betatron functions especially at the dipole magnet.

The tunability is also important to adjust the vertical and horizontal betatron tunes independently. As all dipole magnets are serially connected and excited by the discharge of the capacitor bank, the dipole current cannot be controlled except for the peak current [5]. It means that the tracking between the dipole and focusing magnetic fields must be done by adjusting the focusing magnets.

From the above considerations the proton ring is made of four triplets, each having three quadrupole magnets separated by the long straight section, as shown in Fig. 1.

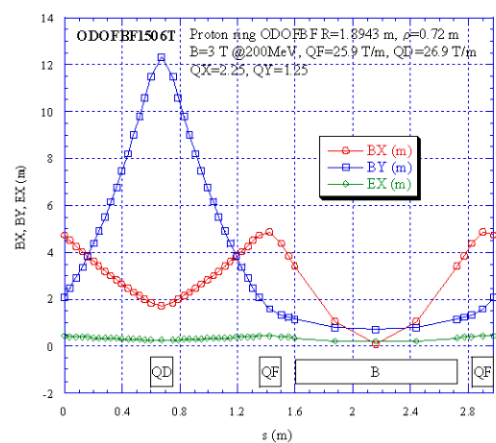


Figure 1: The horizontal and vertical betatron function (BX and BY, respectively), and the horizontal dispersion function (EX) of the proton ring.

2.2 Lattice of the heavy ion ring

The above mentioned lattice design criteria are also applied to the heavy ion ring. Main features of the heavy ion ring different from the proton ring are

- Higher dipole field is adopted to reduce the circumference and to realize the beam parameters similar to the proton ring, and
- Two RF cavities, which are almost the same structure as the proton ring, are used because the charge to mass ratio of the heavy ion is almost half of the proton.

The heavy particle to be accelerated is carbon which is now considered as the most promising ion in the radiation therapy. Therefore, the development of the compact new heavy ion injector is underway in this project. The beam parameters of the heavy ion synchrotron are shown in Fig. 2.

In both rings, the lattice structure is almost same but the circumference is larger by 40% for the heavy ion ring. The differences between these rings are given in Table 1

* kuninori.endo@kek.jp

and layouts of both rings are shown in Fig.3 with the same scale for a quarter of the rings.

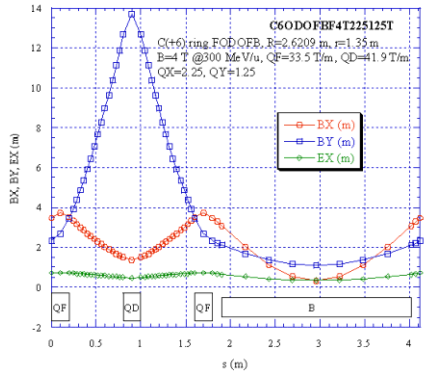


Figure 2: The horizontal and vertical betatron function (BX and BY, respectively), and the horizontal dispersion function (EX) of the heavy ion ring.

Table 1: Machine parameters of the proton and heavy ion synchrotrons

| | Proton ring | C ⁶⁺ ring |
|-------------------------|-------------|----------------------|
| Max. energy | 200 MeV | 300 MeV/u |
| Inj. energy | 2 MeV | ≥ 2 MeV/u |
| Av. beam current (1 Hz) | 20 nA | 0.2 nA |
| Circumference | 11.9 m | 16.5 m |
| Av. radius | 1.89 m | 2.62 m |
| Bending radius | 0.72 m | 1.35 m |
| Tune (Hor/Ver) | 2.25 / 1.25 | 2.25 / 1.25 |
| Max. dispersion | 0.43 m | 0.73 m |
| Tr. energy | 2.29 GeV | 2.08 GeV/u |
| Lattice structure | FODOFB | FODOFB |
| Long straight section | 0.6 m x 8 | 0.6 m x 8 |
| Short straight section | 0.1 m x 8 | 0.1 m x 8 |
| Superperiod | 4 | 4 |

3 MAGNET SYSTEM

The first stage of the development is focused on the verification of the compact proton synchrotron. So the following descriptions only apply for it. However, the every component developed at this stage except for the dipole magnet is reused directly or after a slight modification.

3.1 Dipole magnet

The size of the dipole magnet depends almost on the horizontal beam aperture, but the aperture and the injection energy determine the strength of the circulating beam current. As for the low injection energy as in the present case, it is inevitable to sacrifice protons with large momentum deviation. The practical threshold is set at ±1.5% to limit the beam aperture of ±35 mm at the dipole magnet. With these parameters the average therapeutic proton current of 20 nA will be obtained by the repetition rate of 1 Hz. The model dipole designed so far is shown in Fig.4. and Fig.5.

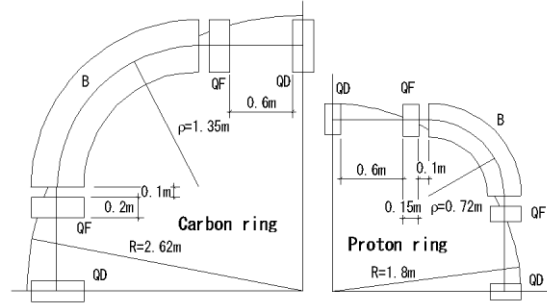


Figure 3: Layouts of the proton (right) and heavy ion (left) rings with the same scale for a quarter of the rings.

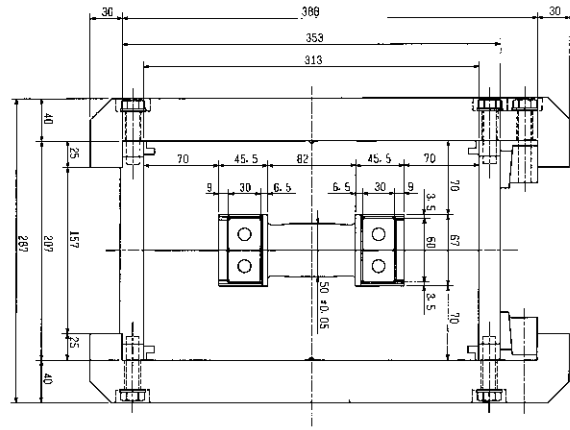


Figure 4: Cross-sectional view of the dipole magnet.

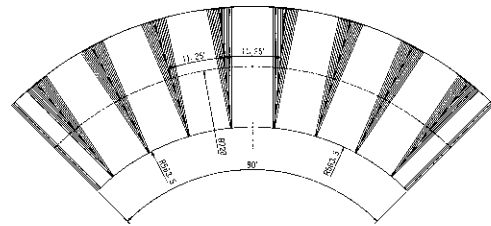


Figure 5: Lamination stacking of the dipole magnet.

The transient 3D field of the dipole magnet is shown in Fig.6 where the normalized radial distributions of the vertical field component (B_y) at every 0.5 ms step are given for a case without the single turn/pole correction coil. Under the pulse excitation of the single turn correction coil it is possible to compensate the sextupole component at the low field.

3.2 Quadrupole magnet

Quadrupoles having the length of 0.14 m are excited up to 30 T/m at maximum. The horizontal and vertical tunes are 2.25 and 1.25, respectively, to obtain a larger dynamic aperture. Under these conditions the fast beam extraction will be made vertically. The preliminary design is given in

Fig. 7. Estimated effective quadrupole length decreases by about 2 mm during acceleration up to 200 MeV.

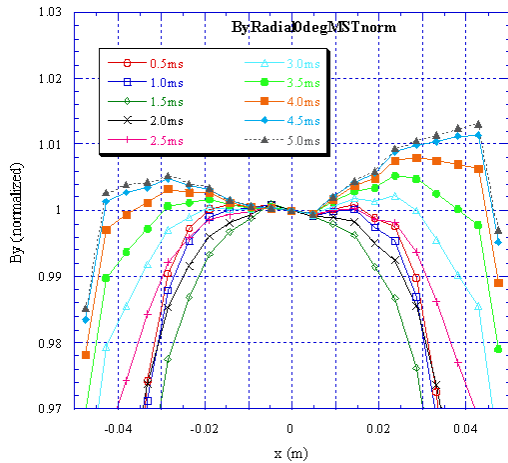


Figure 6: Radial distribution of the normalized vertical field component without a correction coil.

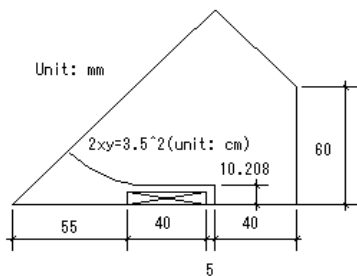


Figure 7: Cross-sectional view of a quadrupole octant.

4 RF SYSTEM

To realize the lattice shown in Fig.1 and Fig.2, a short RF cavity less than 0.5 m in length must be developed. By adopting the micro-crystalline iron alloy (FINEMET), a small RF cavity composed of several short units (Fig.8), each having an accelerating gap, is being manufactured [6]. For this structure it is possible to obtain 5 kV at each gap with the bandwidth from 1.6 MHz to more than 15 MHz. A set of four gap cavity of 0.5 m in length is used for the proton ring and two sets will be used for the heavy ion ring.

5 BEAM SIMULATION

Just after injection at 2 MeV, protons with different momentum are traced under the influence of the RF field and their transverse excursions are simulated assuming the sextupole error field in the dipole magnets. If it is corrected completely by the sextupole magnets, protons with momentum within $\pm 1.5\%$ will remain in the aperture. Otherwise, the beam brows up beyond the aperture limit.

The longitudinal behaviour is also simulated for protons injected all around the ring with initial momentum spread of $\pm 0.2\%$. About 50% protons are trapped for acceleration by transposing an appropriate amount of the 2-nd

harmonics but the 3-rd harmonics leads to the beam loss due to the increased momentum spread as shown in Fig. 9.



Figure 8: Multi-gap RF cavity.

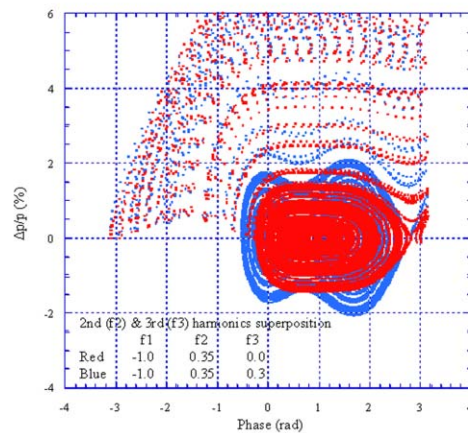


Figure 9: Effect of the superposed 2-nd and 3-rd harmonics. By superposing the 3-rd harmonics, the momentum spread increases.

Authors cordially thank Professor Y. Hirao and Dr. S. Yamada of NIRS for the continuous support to this work.

6 REFERENCES

- [1] I.I. Averboukh et al, "Project of Small-Dimensional 200 MeV Proton Synchrotron," EPAC88, Rome, pp.413-6.
- [2] L. Picardi et al, "Preliminary Design of a Technologically Advanced and Compact Synchrotron for Proton Therapy," Int. Rep. RT/INN/94/20, 1994.
- [3] K. Endo et al, "Table-Top Proton Synchrotron Ring for Medical Applications," EPAC2000, Vienna, pp.2515-7.
- [4] K. Endo et al, "Compact Proton and Heavy Ion Synchrotron for Cancer Therapy and Bio-Science," Proc. 4-th Sym. Acc. Sc. and Tech., 2001, Osaka, pp.426-8.
- [5] K. Endo et al, "Resonant Pulse Power Supply for Compact Proton and/or Heavy Ion Synchrotron," Proc. APAC2001, Beijing, pp.636-8.
- [6] Z. Fang et al, "A Broadband High Gradient RF Cavity for a Compact Proton Synchrotron," this conference.